

---

**Research Articles: Cellular/Molecular**

## **Activating Transcription Factor 4 (ATF4) regulates neuronal activity by controlling GABA<sub>B</sub>R trafficking**

**Carlo Corona<sup>1</sup>, Silvia Pasini<sup>1</sup>, Jin Liu<sup>1</sup>, Fatou Amar<sup>1</sup>, Lloyd A Greene<sup>1</sup> and Michael L Shelanski<sup>1</sup>**

<sup>1</sup>*Department of Pathology & Cell Biology and the Taub Institute for Research on Alzheimer's Disease and the Aging Brain, Columbia University Medical Center, New York, NY, 10033*

DOI: 10.1523/JNEUROSCI.3350-17.2018

Received: 27 November 2017

Revised: 29 May 2018

Accepted: 31 May 2018

Published: 6 June 2018

---

**Author contributions:** M.S. and L.A.G. designed research; M.S. and L.A.G. wrote the paper; C.C., S.P., J.L., and F.A. performed research; C.C., S.P., J.L., and F.A. analyzed data.

**Conflict of Interest:** The authors declare no competing financial interests.

We thank Drs. Ottavio Arancio and Asa Abeliovich for providing equipment for electrophysiological experiments. This work was supported in part by grants from the NIH-NINDS (R01NS033689 and R01NS072050), by the Taub Institute for Research in Alzheimer's disease and by the Marilyn and Henry Taub Foundation.

Corresponding author: Michael L Shelanski, [mis7@columbia.edu](mailto:mis7@columbia.edu)

**Cite as:** J. Neurosci ; 10.1523/JNEUROSCI.3350-17.2018

**Alerts:** Sign up at [www.jneurosci.org/cgi/alerts](http://www.jneurosci.org/cgi/alerts) to receive customized email alerts when the fully formatted version of this article is published.

Accepted manuscripts are peer-reviewed but have not been through the copyediting, formatting, or proofreading process.

Copyright © 2018 the authors

1 **Title:** Activating Transcription Factor 4 (ATF4) regulates neuronal activity by controlling GABA<sub>B</sub>R  
2 trafficking

3 **Abbreviated title:** ATF4 regulates neuronal excitability via GABA<sub>B</sub>Rs

4 **Author names and affiliation:** Carlo Corona<sup>1</sup>, Silvia Pasini<sup>1,2</sup>, Jin Liu<sup>1</sup>, Fatou Amar<sup>1</sup>, Lloyd A  
5 Greene<sup>1</sup>, and Michael L Shelanski<sup>1</sup>

6 <sup>1</sup> Department of Pathology & Cell Biology and the Taub Institute for Research on Alzheimer's  
7 Disease and the Aging Brain, Columbia University Medical Center, New York, NY, 10033

8 <sup>2</sup> Present address: Department of Ophthalmology and Visual Science, Vanderbilt University  
9 Medical Center, Nashville, TN

10 **Corresponding author:** Michael L Shelanski, mls7@columbia.edu

11 **Number of pages:** 16

12 **Number of figures:** 7

13 **Number of words:** Abstract=250, Introduction=509, and Discussion=1140

14 **Conflict of Interest:** Authors declare no conflict of interests

15 **Acknowledgements:** We thank Drs. Ottavio Arancio and Asa Abeliovich for providing equipment  
16 for electrophysiological experiments. This work was supported in part by grants from the NIH-  
17 NINDS (R01NS033689 and R01NS072050), by the Taub Institute for Research in Alzheimer's  
18 disease and by the Marilyn and Henry Taub Foundation.

19

## 20 **ABSTRACT**

21 Activating Transcription Factor 4 (ATF4) has been postulated as a key regulator of learning and  
22 memory. We previously reported that specific hippocampal ATF4 down-regulation causes deficits  
23 in synaptic plasticity and memory and reduction of glutamatergic functionality. Here we extend  
24 our studies to address ATF4's role in neuronal excitability. We find that long-term ATF4  
25 knockdown in cultured rat hippocampal neurons significantly increases the frequency of  
26 spontaneous action potentials. This effect is associated with decreased functionality of  
27 metabotropic GABA<sub>B</sub> receptors (GABA<sub>B</sub>Rs). Knocking down ATF4 results in significant reduction  
28 of GABA<sub>B</sub>R-induced GIRK-currents and increased mIPSCs frequency. Furthermore, reducing  
29 ATF4 significantly decreases expression of membrane-exposed, but not total, GABA<sub>B</sub>R 1a and  
30 1b subunits, indicating that ATF4 regulates GABA<sub>B</sub>R trafficking. In contrast, ATF4 knockdown has  
31 no effect on surface expression of GABA<sub>B</sub>R2s, several GABA<sub>B</sub>R-coupled ion channels or  $\beta$ 2 and  
32  $\gamma$ 2 GABA<sub>A</sub>Rs. Pharmacologic manipulations confirmed the relationship between GABA<sub>B</sub>R  
33 functionality and action potential frequency in our cultures. Specifically, the effects of ATF4 down-  
34 regulation cited-above are fully rescued by transcriptionally active, but not by transcriptionally-  
35 inactive, shRNA-resistant, ATF4. We previously reported that ATF4 promotes stabilization of the

36 actin-regulatory protein Cdc42 by a transcription-dependent mechanism. To test the hypothesis  
37 that this action underlies the mechanism by which ATF4 loss affects neuronal firing rates and  
38 GABA<sub>B</sub>R trafficking, we down-regulated Cdc42 and found that this phenocopies the effects of  
39 ATF4 knockdown on these properties. In conclusion, our data favor a model in which ATF4, by  
40 regulating Cdc42 expression, affects trafficking of GABA<sub>B</sub>Rs, which in turn modulates the  
41 excitability properties of neurons.

42

43 **Significance statement:** GABA<sub>B</sub> receptors (GABA<sub>B</sub>Rs), the metabotropic receptors for the  
44 inhibitory neurotransmitter GABA, have crucial roles in controlling the firing rate of neurons.  
45 Deficits in trafficking/functionality of GABA<sub>B</sub>Rs have been linked to a variety of neurological and  
46 psychiatric conditions, including epilepsy, anxiety, depression, schizophrenia, addiction, and pain.  
47 Here we show that GABA<sub>B</sub>Rs trafficking is influenced by Activating Transcription Factor 4 (ATF4),  
48 a protein that has a pivotal role in hippocampal memory processes. We found that ATF4 down-  
49 regulation in hippocampal neurons reduces membrane-bound GABA<sub>B</sub>R levels and thereby  
50 increases intrinsic excitability. These effects are mediated by loss of the small GTPase Cdc42  
51 following ATF4 down-regulation. These findings reveal a critical role for ATF4 in regulating the  
52 modulation of neuronal excitability by GABA<sub>B</sub>Rs.

53

#### 54 **Introduction**

55 Normal cognitive functions rely on the balance of neuronal excitability properties throughout the  
56 brain as well as on synaptic plasticity (Beck and Yaari, 2008). Among the many proteins reported  
57 to influence cognition, mounting evidence suggests a pivotal role for Activating Transcription  
58 Factor 4 (ATF4), an ubiquitously expressed member of the ATF/CREB transcription factor family  
59 of basic leucine zipper proteins. In addition to its well-known functions as a stress-induced protein  
60 (Ameri and Harris, 2008), a number of studies have implicated ATF4 in synaptic plasticity and in  
61 learning and memory. Depending on cellular context, ATF4 has been characterized as either an  
62 inhibitor or promoter of synaptic plasticity (Pasini et al., 2015). Similarly divergent suggestions  
63 about ATF4's functions in learning and memory have been advanced, but these are largely based  
64 on indirect and non-selective manipulation of ATF4 activity or expression (Chen et al., 2003;  
65 Costa-Mattioli et al., 2007). To probe directly ATF4's role in normal brain function, we have  
66 monitored the consequences of its knockdown or knockout in neuronal culture and in animals.  
67 This has led to observations that ATF4 plays a role in regulation of mushroom dendritic spine  
68 density as well as in synaptic glutamatergic function (Liu et al., 2014). These effects appeared to  
69 be due to ATF4's direct transcriptional regulation of RhoGDI $\alpha$  (product of the *Arhgdia* gene), which  
70 in turn affects stability of the Rho family member Cdc42 that is involved in regulation of the actin  
71 cytoskeleton (Pasini et al., 2016). At the physiological level, loss of ATF4 manifested in reduced  
72 frequency and amplitude of mEPSCs, followed by defective LTP and LTD as well as in memory  
73 deficits (Pasini et al., 2015). Of relevance, similar deficiencies in plasticity and memory have been  
74 observed after conditional Cdc42 knockout in brain (Kim et al., 2014). In the context of ATF4's  
75 role in neuronal functionality, one area of interest is in its relation to GABA<sub>B</sub> receptors (GABA<sub>B</sub>Rs),  
76 the G-protein-linked metabotropic receptors for the inhibitory neurotransmitter GABA. Several

77 studies have shown direct association of GABA<sub>B</sub>Rs with ATF4 (Nehring et al., 2000; White et al.,  
 78 2000; Vernon et al., 2001; Ritter et al., 2004) while another study reported that ATF4 differentially  
 79 regulates activity of promoters for the GABA<sub>B</sub>Rs subunits 1a and 1b (Steiger et al., 2004).  
 80 GABA<sub>B</sub>Rs are widely expressed in brain and regulate neuronal excitability by modulating activity  
 81 of G protein-gated inwardly rectifying K<sup>+</sup> channels (GIRKs), voltage-gated Ca<sup>2+</sup> channels and  
 82 adenylyl cyclase (Gassmann and Bettler, 2012). Activation of GABA<sub>B</sub>Rs has been reported to  
 83 hyperpolarize and decrease the threshold, while deactivation of the receptors increases the  
 84 threshold required to generate an action potential (Ladera et al., 2008). Thus, alterations of  
 85 GABA<sub>B</sub>R trafficking/functionality have the potential to significantly alter intrinsic neuronal  
 86 excitability and brain function. In this work, we have investigated the role of ATF4 in neuronal  
 87 excitability. We find that ATF4 knockdown in cultured hippocampal neurons significantly increases  
 88 their firing rate and that this appears to be due to reduced trafficking of GABA<sub>B</sub>R to the cell surface.  
 89 These effects in turn appear to be a consequence of ATF4's regulation of Cdc42 stability.

## 90 **Methods**

### 91 Cell cultures

92 Primary hippocampal cultures were prepared as previously described (Liu et al., 2015). Briefly,  
 93 hippocampi were dissected from E18 rat embryos of either sex and, after dissociation, neurons  
 94 were plated on poly-D-lysine-coated 12-well-plates at the density of  $3 \times 10^5$  cells/well. Neurons  
 95 were maintained in Neurobasal medium (Invitrogen) supplemented with 2% B-27 (Invitrogen) and  
 96 0.5 mM glutamine (Invitrogen). Elisa measurements of both cell media and cell lysates revealed  
 97 the presence of both GABA and glutamate in the culture (glutamate=32.2  $\mu$ g, GABA=13.9  $\mu$ g).

98

### 99 DNA constructs, lentivirus preparation and infection

100 All shRNAs were cloned in the pLVTHM vector (Addgene), which contains an EF-1 $\alpha$  promoter for  
 101 target gene expression, using the following oligo DNA pairs as previously described (Liu et al.,  
 102 2014).

103 Lenti-shRNA control:

104 5'-CGCGTCACAGCCCTTCCACCTCCATTCAAGAGATGGAGGTGGAAGGGCTGTGTTTTTT

105 A-3' and 5'-CGCGTAAAAAACACAGCCCTTCCACCTCCATCTCTTGAATGGAGGTGGA  
 106 AGGGCTGTGA-3'.

107 Lenti-shATF4:

108 5' -CGCGTGCCTGACTCTGCTGCTTATTTCAAGAGAATAAGCAGCAGAGTCAGGC

109 TTTTTTA-3' and 5' -CGCGTAAAAAAGCCTGACTCTGCTGCTTATTCTCTTGAA

110 ATAAGCAGCAGAGTCAGGCA-3'

111 Lenti-shATF4 addback was generated using the QuickChange Site-directed Mutagenesis kit  
112 (Stratagene). Point mutations were introduced into the Lenti-ATF4 at the recognition site for  
113 shATF4 (CCTGACTCTGCTGCTTAT to CCAGAGTCAGCTGCTTAC).

114 Lenti-shATF4 mut/addback was generated from shATF4addback by introducing point mutations  
115 at the DNA binding site (292RYRQKKR298 to 292GYLEAAA298).

116 Lenti-shCdc42 was generated according to a published siRNA sequence 5'-  
117 GAUAACUCACCACUGUCCATT-3' (Deroanne et al., 2005). A scrambled shRNA (lenti-  
118 shCdc42scr) was generated by using the following oligo DNA pair: 5'-  
119 CGCGTGTCCAACGTCCATATACCATTCAAGAGATGGTATATGGACGTTGGACTTTTTTA-3'  
120 and 5'-CGCGTAAAAAAGTCCAACGTCCATATACCATCTCTTGAATGGTATATGGACGTTG G  
121 ACA-3'. Lentiviral particles were produced using the 2<sup>nd</sup> generation packaging system. Briefly,  
122 HEK293T cells were transfected with the respective lentiviral constructs for shRNA together with  
123 the packaging vectors psPAX2 and pMD2.G (Addgene) using calcium phosphate. Two and three  
124 days after transfection, cell supernatants were collected and lentiviral particles were concentrated  
125 20–30x by centrifugation in Amicon Ultra centrifugal filters (100KD) (Millipore). Viral titer ranged  
126 between 1–5×10<sup>6</sup> virions/μl. Primary neuronal cultures were infected with viral particles on *Day In*  
127 *Vitro* 7 (*DIV*7) and RNA and protein extraction were performed at the indicated time points.

128

#### 129 RNA Extraction and Quantitative RT-PCR

130 Total RNA was extracted from rat primary hippocampal cultures 4, 8, and 12 days after lentiviral  
131 infection according to the RNeasy Mini Protocol (Quiagen kit). RNA concentration and purity were  
132 determined using a NanoDrop 8000 (Thermo Scientific, Wilmington, DE). mRNA was then  
133 reverse-transcribed into cDNA using the 1<sup>st</sup> Strand cDNA Synthesis System for quantitative RT-  
134 PCR (Origene) following the manufacturer's instructions. Reaction mixtures were diluted 5-fold  
135 and subjected to qRT-PCR amplification (Eppendorf) using FastStart SYBR Green Master mix  
136 (Roche). The following primers were used: ATF4: F 5'-ATGCCAGATGAGCTCTTGACCAC-3' and  
137 R 5'-GTCATTGTCAGAGGGAGTGTCTTC-3'; αTubulin: F 5'-TACACCATTGGCAAGGAGAT-3'  
138 and R 5'-GGCTGGGTAAAT GGAGAACT-3; GABA<sub>B</sub>R 1a: F 5'-CACACCCAGTCGCTGTG-3' and  
139 R 5'-GAGGTCCCCACCCGTCA-3'; GABA<sub>B</sub>R 1b 5'-GGGACCCTGTACCCCGGTG-3' and R 5'-  
140 GGAGTGAGAGGCCACACC-3'. Relative product quantities for each transcript were performed  
141 in triplicate, normalized to αTubulin mRNA as an endogenous control, and determined using the  
142 comparative CT method.

143

#### 144 Electrophysiology

145 Primary hippocampal neurons (19-21 *DIV*, 2 weeks after lentiviral infection) were used for tight  
146 seal conventional whole-cell patch clamp. All the currents were recorded from pyramidal-like  
147 neurons, based on their large (~15μm) triangular shaped somas. Coverslips were placed in a  
148 recording chamber with bath solution containing (in mM): 119 NaCl, 5 KCl, 20 Hepes, 30 glucose,  
149 2 CaCl<sub>2</sub>, 2 MgCl<sub>2</sub>. The pH and osmolarity of the bath solution were adjusted to 7.3 and 330

150 mOsm/L, respectively. For spontaneous action potential recordings, glass pipettes were filled with  
151 intracellular electrode solution (pH 7.3, 285 mOsm/L) containing (in mM): 130 K-gluconate, 10  
152 KCl, 10 HEPES, 1 MgCl<sub>2</sub>, 0.06 CaCl<sub>2</sub>, 0.1 EGTA, 3 MgATP, 0.3 Na<sub>2</sub>GTP, and typically registered  
153 4–8 MΩ pipette resistances. Following acquisition of electrical access, cells were held in current-  
154 clamp mode at I=0. For mIPSCs experiments, glass pipettes were filled with intracellular electrode  
155 solution (pH 7.3, 285 mOsm/L) containing (in mM): 130 KCl, 10 Hepes, 0.5 CaCl<sub>2</sub>, 1 EGTA, 3  
156 MgATP, 0.3 Na<sub>2</sub>GTP. Furthermore, 1 μM TTX, 10 μM CNQX, and 50 μM D-APV were  
157 continuously perfused during the experiment. All the cells were recorded at -70 mV for 10 min  
158 and a 5 mV hyperpolarizing test pulse was applied periodically during recordings to ensure that  
159 the access resistance did not change significantly and was less than 25 MΩ. If not, the recordings  
160 were discarded. Signals were filtered at 2 kHz, digitized at 10 kHz, stored and analyzed offline  
161 using MiniAnalysis Software (Synaptosoft, Version 6.0.7). The threshold for event detection was  
162 set at 5 pA. Recordings were performed at room temperature under constant perfusion (2 mL/min)  
163 and acquired using Clampex software and a microamplifier (MultiClamp 700B, Molecular  
164 Devices). For Baclofen-induced GIRK currents, hippocampal neurons were bathed initially with a  
165 solution containing (in mM) 119 NaCl, 5 KCl, 20 Hepes, 30 glucose, 2 CaCl<sub>2</sub>, 2 MgCl<sub>2</sub> (pH 7.3,  
166 330 mOsm/L) and then switched to a high potassium solution (hK) containing (in mM) 85 NaCl,  
167 60 KCl, 2 MgCl<sub>2</sub>, 2 CaCl<sub>2</sub>, 10 Hepes, 10 Glucose (pH 7.3) to determine the amplitude of the basal  
168 potassium current. When the basal current reached equilibrium, Baclofen diluted in hK  
169 was applied. The hK induced current was subtracted from the total current to obtain the Baclofen-  
170 induced GIRK current. Membrane potential was held at -70 mV throughout the duration of the  
171 experiment.

#### 172 Surface and total protein isolation

173 Membrane-bound and total protein isolation was conducted using the EZ-Link NHS-PEO4-  
174 Biotinylation Kit (Pierce), following manufacturer's instructions. Briefly, cells were gently washed  
175 three times with ice-cold PBS containing 1 mM MgCl<sub>2</sub> and 0.1 mM CaCl<sub>2</sub> (PBS/CM) and then  
176 incubated with 500 μg/ml of EZ-link NHS-PEO4-biotin dissolved in ice-cold PBS at 4°C for 1 hour.  
177 Cells were then washed once with ice-cold PBS and the reaction quenched by adding 500 μl of  
178 100 mM glycine for 10 minutes, followed by 3 washes in ice-cold-PBS. Cells were then harvested  
179 in RIPA buffer supplemented with protease/phosphatase inhibitor and centrifuged at 14000 rpm  
180 for 15 minutes at 4°C. 30 μl of the resulting supernatant were collected for total protein input and  
181 the rest incubated with 50 μg of streptavidin beads, rotating overnight at 4°C. Beads were washed  
182 5 times with RIPA buffer and bound proteins eluted with 1x sample buffer by boiling for 5 minutes.

#### 183 Immunoblotting

184 After adding NuPAGE LDS Sample Buffer (Invitrogen) and 5% β-mercaptoethanol, samples were  
185 boiled for 15 min and proteins were separated by electrophoresis on 4-12% BisTris SDS-  
186 acrylamide gels (Invitrogen). After transfer, the membranes were blocked for 1 hour at room  
187 temperature with 5% milk and then incubated overnight with primary antibody. The following  
188 primary antibodies were used: rabbit anti-GABA<sub>B</sub> R1 (1:1000, Abcam, #55051 (Zapata et al.,  
189 2017)), GABA<sub>B</sub> R2 (1:1000, Cell Signaling, #3839), rabbit anti-GABA<sub>A</sub>R β2 (1:1000, Synaptic  
190 Systems, #224803), rabbit anti-GABA<sub>A</sub>R γ2 (1:1000, Synaptic Systems, #224003), rabbit anti-

191 ATF4 (1:1000, Cell Signaling, #11815), rabbit anti-Cdc42 (1:1000, Cell Signaling, #2462S), rabbit  
192 anti-GIRK1 (1:500, Abcam, #129182), rabbit anti-GIRK2 (1:200, Sigma-Aldrich, #P8122), rabbit  
193 anti-GIRK3 (1:400, Sigma-Aldrich, #P8247), mouse anti-GAPDH (1:10000, Invitrogen, #MA1-  
194 16757), rabbit anti-K<sub>v</sub>1.1 (1:400, Sigma-Aldrich, #P8247), mouse anti-K<sub>v</sub>2.1 (1:500, Abcam,  
195 #ab192761), rabbit anti-K<sub>v</sub>4.2 (1:200, Sigma-Millipore, #07-491), rabbit anti-Ca<sub>v</sub>2.1 (1:500,  
196 abcam, #ab32642). Densitometric quantification of the bands was performed using ImageJ  
197 software (NIH). Total level of proteins (input) was normalized to GAPDH, while membrane-bound  
198 samples were normalized with the ratio input/GAPDH. GAPDH was undetectable in the  
199 membrane-bound fraction, therefore excluding the possibility that the membrane was leaky or  
200 compromised.

201 Statistical analysis

202 Data are shown as means  $\pm$  SEM. Comparison between two groups was performed with a two-  
203 tailed unpaired Student's t test. Comparison between multiple groups was performed using two-  
204 way ANOVA, followed by a Bonferroni *post hoc* test when applicable. Statistical significance was  
205 set at  $p < 0.05$ .

206

## 207 Results

208

### 209 ATF4 knockdown increases neuronal excitability

210 We previously described a key role for ATF4 in modulating glutamatergic neurotransmission both  
211 *in vitro* and *in vivo* and in regulating dendritic spines (Liu et al., 2014; Pasini et al., 2015). Given  
212 the pivotal roles of these two aspects in controlling the excitability properties of neurons, we next  
213 set out to directly investigate the role of ATF4 in intrinsic neuronal excitability. For this purpose,  
214 we used lentivirally delivered shRNAs to specifically down-regulate ATF4 expression in 7 DIV  
215 cultured rat hippocampal neurons and performed whole-cell patch-clamp two weeks after the  
216 infection to record the frequency of spontaneously-occurring action potentials (sAPs). At this time  
217 in culture (3 weeks total), the neurons have formed extensive synaptic connections (Liu et al.,  
218 2014). As shown in Figure 1A,B, knockdown of ATF4 resulted in an approximately 3-fold increase  
219 in the frequency of sAPs compared to neurons infected with a control shRNA  
220 (shCtrl=0.35 $\pm$ 0.07Hz, shATF4=1.11 $\pm$ 0.26Hz; *post hoc* Bonferroni, shCtrl vs shATF4  $p < 0.01$ ) To  
221 confirm that this result was not due to off-target effects, we performed a rescue experiment in  
222 which the neurons were co-infected with lentiviruses expressing shATF4 and an ATF4 construct  
223 (ATF4add) conservatively mutated to make it unresponsive to shATF4. This resulted in  
224 knockdown of endogenous and overexpression of exogenous ATF4, respectively (Liu et al.,  
225 2014). Our results indicate that ATF4add restored the firing rate to the control level (Fig. 1A,B;  
226 shATF4+ATF4add=0.46 $\pm$ 0.07Hz; *post hoc* Bonferroni, shCtrl vs shATF4+ATF4add,  $p > 0.05$ ).  
227 However, while ATF4 over-expression rescued the firing rate, it did not reduce it below that seen  
228 in control cultures. Next, to test whether the effects of ATF4 on sAP frequency requires its  
229 transcriptional activity, we co-infected cultured hippocampal neurons with shATF4 and a mutant

230 ATF4 construct, ATF4add/mut, that is not recognized by shATF4 and that encodes a mutant ATF4  
231 that does not bind DNA and thus is transcriptionally inactive. This results in knockdown of  
232 endogenous ATF4 and overexpression of inactive exogenous ATF4 (Liu et al., 2014). In contrast  
233 to ATF4add, ATF4add/mut failed to rescue the effect of ATF4 knockdown (Fig. 1A,B;  
234 shATF4+ATF4add/mut=1.17±0.21Hz; *post hoc* Bonferroni, shCtrl vs shATF4+ATF4add/mut,  
235  $p<0.01$ ), suggesting that ATF4 must retain its transcriptional capability to regulate the frequency  
236 of neuronal firing. Because APs are generated by voltage-gated sodium ( $Na_v$ ) and potassium ( $K_v$ )  
237 channels (Bean, 2007), we investigated whether ATF4 down-regulation could affect the neuronal  
238 firing rate by influencing these major AP constituents. However, our results show no differences  
239 in either  $Na_v$  or  $K_v$  I-V curves obtained from shCtrl- or shATF4-infected hippocampal cultures (Fig.  
240 1C-E), suggesting that ATF4 regulates neuronal excitability by a mechanism independent of  
241 effects on  $Na_v$  or  $K_v$ .

#### 242 **ATF4 regulates trafficking of GABA<sub>B</sub>Rs to the membrane**

243 Among the many proteins reported to modulate the excitability of neurons, we focused on GABA<sub>B</sub>  
244 receptors (GABA<sub>B</sub>Rs), the metabotropic (G-protein coupled) receptors for GABA. Postsynaptic  
245 GABA<sub>B</sub>Rs induce a slow inhibitory postsynaptic current (sIPSC) by gating Kir-type  $K^+$ -channels.  
246 This in turn hyperpolarizes the membrane and shunts excitatory currents, thereby inhibiting  
247 generation of action potentials (Leung and Peloquin, 2006). In this light, we confirmed that  
248 blocking GABA<sub>B</sub>R activity in our cultures increases the neuronal firing rate. As shown in Figure  
249 2A, application of the specific GABA<sub>B</sub>R antagonist CGP55845 (10  $\mu$ M) produced a rapid 8-fold  
250 rise (from about 0.4 to 3.2 Hz) of sAP frequency. Of potential relevance, ATF4 has been reported  
251 to directly bind GABA<sub>B</sub>Rs as well as to differentially regulate promoter activity of the subunits 1a  
252 and 1b of GABA<sub>B</sub>Rs (Steiger et al., 2004). We therefore first investigated whether ATF4 down-  
253 regulation affects expression of GABA<sub>B</sub>Rs at the transcriptional level. To achieve this, we infected  
254 cultured hippocampal neurons with either shATF4 or shCtrl for 4-15 days and then carried out  
255 qRT PCR. As shown in Figure 2B, knockdown of ATF4 did not significantly affect the transcript  
256 levels of either GABA<sub>B</sub>R 1a or 1b subunits (ATF4, 4 days: shCtrl=100±7.1%, shATF4=19.1±2.4%,  
257 t test  $p<0.01$ ; ATF4, 8 days: shCtrl=100±3%, shATF4=11.6±2.8%, t test  $p<0.01$ ; ATF4, 12 days:  
258 shCtrl=100±4.19%, shATF4=9.47±1.63%, t test  $p<0.01$ ).

259 Next we determined whether knocking down ATF4 would alter total or membrane- bound protein  
260 expression of GABA<sub>B</sub>Rs. To achieve this, we performed biotinylation of plasma membrane  
261 proteins on cultured hippocampal neurons with or without ATF4 knockdown (infected at 7 *DIV* for  
262 2 weeks), isolated the biotinylated proteins on streptavidin-bound beads and carried out western  
263 immunoblotting analysis for GABA<sub>B</sub>R subunits 1a and 1b on both the input (total cell lysate) and  
264 membrane fractions. Densitometric quantification from multiple experiments showed that ATF4  
265 down-regulation did not affect total GABA<sub>B</sub>R 1a and 1b protein levels (Fig. 2C), but significantly  
266 decreased the levels of GABA<sub>B</sub>R subunits 1a and 1b in the biotinylated membrane fraction (Fig.  
267 2C; GABA<sub>B</sub>R 1a: shCtrl=100±11.8%, shATF4=46.7±10.7%; *post hoc* Bonferroni test: shCtrl vs  
268 shATF4  $p<0.01$ ; GABA<sub>B</sub>R 1b: shCtrl=100±7.2%, shATF4=48.2±7.9%; *post hoc* Bonferroni test:  
269 shCtrl vs shATF4  $p<0.01$ ) thus indicating a role for ATF4 in regulating GABA<sub>B</sub>R trafficking, but not  
270 overall expression.



271 To address the question of whether the effect of ATF4 on membrane trafficking of GABA<sub>B</sub>Rs  
272 involves ATF4's transcriptional activity, we performed a rescue experiment as above and found  
273 that ATF4add/mut, in contrast to ATF4add, failed to reverse the effects of ATF4 knockdown (Fig.  
274 2C; GABA<sub>B</sub>R 1a, shATF4+ATF4add=95.1±10.3%, shATF4+ATF4add/mut=39.8±8.2%; *post hoc*  
275 Bonferroni test: shCtrl vs shATF4+ATF4add  $p>0.05$ , shATF4 vs shATF4+ATF4add  $p<0.05$ , shCtrl  
276 vs shATF4+ATF4add/mut  $p<0.01$ . GABA<sub>B</sub>R 1b, shATF4+ATF4add=110.5±12.7%,  
277 shATF4+ATF4add/mut=55.2±10%; *post hoc* Bonferroni test: shCtrl vs shATF4+ATF4add  $p>0.05$ ,  
278 shATF4 vs shATF4+ATF4add  $p<0.001$ , shCtrl vs shATF4+ATF4add/mut  $p<0.05$ ). This indicates,  
279 as with neuronal excitability, that ATF4 has a transcriptional role in regulating trafficking of  
280 GABA<sub>B</sub>Rs. The data also show, as with excitability, that ATF4 over-expression is not sufficient to  
281 drive surface expression of GABA<sub>B</sub>Rs beyond that seen with basal endogenous expression.

282 We next asked whether knocking down ATF4 might produce a more general or non-specific effect  
283 on membrane proteins. Interestingly, both the total and membrane-bound levels of GABA<sub>B</sub>R 2  
284 (biotin labeled as above) were unaffected by ATF4 down-regulation (Fig. 2D). We also examined  
285 the effect of shATF4 on membrane-exposed  $\beta 2$  and  $\gamma 2$  subunits of GABA<sub>A</sub> receptors and found  
286 no effects on either the total or membrane-exposed protein levels (Fig. 3A). In addition to  
287 GABA<sub>B</sub>Rs, a wide variety of voltage-sensitive K and Ca channels has been described to regulate  
288 excitability properties of neurons (Chen et al., 2006; Hsiao et al., 2009; Rossignol et al., 2013;  
289 Specca et al., 2014). We therefore queried whether the effect of ATF4 on neuronal excitability was  
290 in part due to its capability to regulate the expression or localization of K<sub>v</sub>1.1, K<sub>v</sub>2.1, K<sub>v</sub>4.2, and  
291 Ca<sub>v</sub>2.1. As shown in Fig. 3B-E, neither the total nor the membrane-bound levels of these proteins  
292 was affected by ATF4 down-regulation. These findings thus indicate that ATF4 has a selective  
293 role in regulation of membrane-bound proteins involved in neuronal excitability and that this  
294 includes GABA<sub>B</sub>Rs.

#### 295 **ATF4 knockdown reduces GIRK currents**

296 We next queried whether the reduction we observed in the number of membrane-inserted  
297 GABA<sub>B</sub>Rs after ATF4 down-regulation reflected a change in the functionality of the receptors  
298 themselves. Post-synaptic GABA<sub>B</sub>Rs are associated with, and mediate part of their functions  
299 through G protein-coupled inwardly-rectifying potassium (GIRK) channels (Gassmann and  
300 Bettler, 2012). We therefore studied the function of GABA<sub>B</sub>Rs by whole-cell patch-clamp recording  
301 of GABA<sub>B</sub>R-induced K<sup>+</sup> GIRK currents in 7 DIV hippocampal cultured neurons infected for 2 weeks  
302 with lentiviruses carrying either shCtrl or shATF4. As shown in Fig. 4A, we first calibrated our  
303 recordings by applying the GABA<sub>B</sub>R agonist Baclofen (100  $\mu$ M), which elicited sustained K<sup>+</sup>  
304 currents in control neurons that were prevented by pre-treating the cells with a specific GABA<sub>B</sub>R  
305 antagonist (SCH50911, 100  $\mu$ M). Consistent with our finding that ATF4 down-regulation reduces  
306 cell surface GABA<sub>B</sub>R levels, when we recorded Baclofen-induced GIRK currents in ATF4  
307 knockdown neurons, we found them to be significantly reduced when compared to those in ShCtrl  
308 infected neurons (Fig. 4B; shCtrl 725.9±58.4pA, shATF4 435.1±39.2pA; *post hoc* Bonferroni:  
309  $p<0.01$ ). This effect did not appear to be mediated by effects on GIRK channels in that shATF4  
310 did not affect total or membrane-bound GIRK1, GIRK2, or GIRK3 protein levels (Fig. 4C). Finally,  
311 ATF4add, but not ATF4add/mut, completely restored the currents to the control level (Fig. 4B;  
312 shATF4+ATF4add=786.9±69.2pA, shATF4+ATF4add/mut=545.9±43.8pA; *post hoc* Bonferroni:

313 shATF4 vs shATF4+ATF4add,  $p<0.001$ ; shATF4add vs shATF4add/mut,  $p<0.01$ ), further  
314 confirming the idea that ATF4 needs to retain its transcriptional capability to regulate the trafficking  
315 of GABA<sub>B</sub>Rs. As with GABA<sub>B</sub>R membrane trafficking, ATF4 over-expression did not raise GIRK  
316 current amplitude beyond that in control cultures.

#### 317 **ATF4 knockdown increases the frequency, but not amplitude of mIPSCs**

318 Given that GABA<sub>B</sub>R manipulations have been reported to affect the frequency, but not the  
319 amplitude of spontaneous miniature inhibitory postsynaptic currents (mIPSCs; (Ulrich and  
320 Huguenard, 1996; Kubota et al., 2003; Kirmse and Kirischuk, 2006)), we assessed mIPSCs  
321 (confirmed by picrotoxin blockade) in cultured hippocampal neurons infected with either shCtrl or  
322 shATF4 as a further readout of GABA<sub>B</sub>R functionality. As shown in Figure 5A, we found that  
323 shAT4 significantly increases (by about 2-fold) the frequency, but not the amplitude of mIPSCs  
324 (mIPSCs frequency: shCtrl=1.65±0.21Hz, shATF4=3.43±0.41Hz; *post hoc* Bonferroni:  $p<0.05$ ).  
325 In addition, adding back ATF4 completely restored the frequency of mIPSCs to control values  
326 (Fig. 5A; shATF4+ATF4add=1.19±0.37Hz; *post hoc* Bonferroni: shATF4 vs shATF4+ATF4add,  
327  $p<0.05$ ). As with other properties described above, ATF4add overexpression did not increase  
328 mIPSC frequency beyond the level observed in control cultures. Furthermore, our whole-cell  
329 patch-clamp recordings showed that, unlike ATF4add, ATF4add/mut was unable to reverse the  
330 effect of ATF4 down-regulation on mIPSC frequency (Fig. 5A;  
331 shATF4+ATF4add/mut=3.83±0.76Hz; *post hoc* Bonferroni: shCtrl vs shATF4+ATF4add/mut,  
332  $p<0.01$ ), confirming that the transcriptional activity of ATF4 is required for this action. To further  
333 confirm the idea that membrane-bound GABA<sub>B</sub>Rs are reduced by shATF4, we treated both shCtrl  
334 and shATF4-infected neurons with the specific GABA<sub>B</sub>R agonist Baclofen (20 μM) or GABA<sub>B</sub>R  
335 antagonists SCH50911 and CGP55845 (used at 100 and 10 μM, respectively). As shown in Fig.  
336 5B, Baclofen application significantly reduced the frequency of mIPSCs both in shCtrl- and  
337 shATF4-infected hippocampal neurons (shCtrl+Baclofen=0.79±0.14Hz,  
338 shATF4+Baclofen=1.23±0.15Hz; *post hoc* Bonferroni: shCtrl vs shCtrl+Baclofen,  $p<0.05$ ; shATF4  
339 vs shATF4+Baclofen,  $p<0.01$ ), thus confirming that the membrane-bound GABA<sub>B</sub>Rs of shATF4-  
340 infected hippocampal neurons are properly responding to stimulation. Interestingly, the  
341 application of GABA<sub>B</sub>R antagonists CGP55845 and SCH50911 significantly elevated mIPSCs  
342 frequency in shCtrl but not in shATF4 neurons (Fig. 5B; shCtrl+SCH=3.19±0.30Hz,  
343 shCtrl+CGP=3.67±0.46Hz, shATF4+SCH=3.38±0.44Hz, shATF4+CGP=3.59±0.15Hz; *post hoc*  
344 Bonferroni: shCtrl vs shCtrl+SCH,  $p<0.05$ ; shCtrl vs shCtrl+CGP,  $p<0.05$ , shATF4 vs  
345 shATF4+SCH, shATF4 vs shATF4+CGP,  $p>0.05$ ), which is consistent with the observation that  
346 shATF4 reduces membrane-bound levels of GABA<sub>B</sub>Rs. As expected, none of the treatments  
347 significantly affected the amplitude of mIPSCs (Fig. 5B).

#### 348 **The effects of ATF4 on excitability and GABA<sub>B</sub>Rs appear to be mediated by changes in** 349 **Cdc42 expression**

350 We previously reported that ATF4's modulation of dendritic spine density and glutamatergic  
351 functionality is mediated, at least in part, by its capacity to regulate the stability and expression of  
352 the total and activated forms of the small Rho GTPase Cdc42 (Liu et al., 2014; Pasini et al., 2015).  
353 Of particular relevance here, Cdc42 has been shown to be involved in regulating receptor

354 trafficking (Hussain et al., 2015). We therefore next tested the hypothesis that the effects of ATF4  
355 down-regulation on GABA<sub>B</sub>R trafficking and neuronal excitability could be mediated by loss of  
356 Cdc42. To achieve this, we used a previously characterized Cdc42 shRNA (Liu et al., 2014) to  
357 deplete Cdc42 in cultured hippocampal neurons and determined whether this phenocopies the  
358 effects of ATF4 knockdown. We first assessed whether specific Cdc42 down-regulation affects  
359 neuronal excitability. As in the case of ATF4 knockdown, silencing Cdc42 protein produced a 2-  
360 fold increase of AP frequency (Fig. 6A; shCtrl=0.43±0.13Hz, shCdc42=1.08±0.15Hz; t test,  
361 p<0.01). Next we queried whether Cdc42 down-regulation phenocopies the effect of ATF4  
362 knockdown on GABA<sub>B</sub>R trafficking and found that this was sufficient to significantly decrease the  
363 levels of membrane-exposed, but not total GABA<sub>B</sub>Rs (Fig. 6B; for GABA<sub>B</sub>R 1a  
364 shCtrl=100%±23.3%, shCdc42 44.2%±7.4%; t test, p<0.05; GABA<sub>B</sub>R 1b shCtrl=100%±20.3%,  
365 shCdc42 38.7%±4.7%; t test, p<0.05). In addition, we found that Baclofen-induced GIRK currents  
366 were significantly decreased in shCdc42-infected neurons, compared to controls (Fig. 6C;  
367 shCtrl=627.8±77.6pA, shCdc42=406.9±52.9pA; t test, p<0.05). Finally, Cdc42 knockdown also  
368 increased the frequency mIPSCs (Fig. 6D; shCtrl=1.55±0.16Hz, shCdc42=3.21±0.67Hz; t test,  
369 p<0.05) to a degree similar to that observed with ATF4 knockdown. However, with Cdc42  
370 knockdown, there was also a small, but significant increase in mIPSCs amplitude (Fig. 6D;  
371 shCtrl=25.22±1.26pA, shCdc42=31±1.21pA; t test, p<0.01). Taken together, these findings  
372 support the idea that regulation of Cdc42 levels mediates the effects of ATF4 on neuronal  
373 GABA<sub>B</sub>R trafficking and excitability.

#### 374 Discussion

375 In the present study we delineate a novel role for the transcription factor ATF4 in regulating  
376 GABA<sub>B</sub>R trafficking and neuronal excitability. Our data show that chronic ATF4 down-regulation  
377 in hippocampal neurons reduces membrane levels of GABA<sub>B</sub>Rs, diminishes their functionality,  
378 and consequently leads to a substantial increase of neuronal firing rate. In addition, we found that  
379 these effects are mediated by ATF4's transcriptional capability and reflect changes in expression  
380 of the small GTPase Cdc42. Studies on ATF4's role in the regulation of synaptic plasticity and  
381 memory have led to divergent views. ATF4 has been characterized to be either a negative or  
382 positive influence on plasticity. Such interpretations appear to be dependent on cellular context  
383 (Bartsch et al., 1995; Hu et al., 2015) or have been based on experimental manipulations that are  
384 not specific to ATF4 such use of a dominant-negative construct (Chen et al., 2003) or regulation  
385 of eIF2 $\alpha$  phosphorylation (Costa-Mattioli et al., 2007). To more directly assess ATF4's function in  
386 unstressed brain, we have used the strategy of studying the effects of long-term ATF4 knockdown  
387 or deletion in hippocampal and cortical neurons both *in vitro* and *in vivo*. This has revealed  
388 required roles for ATF4 in maintaining mushroom spines and glutamatergic functionality as well  
389 as in long-term spatial memory and behavioral flexibility (Liu et al., 2014; Pasini et al., 2015). The  
390 present findings significantly extend the range of cognition-relevant neuronal properties that are  
391 dependent on the presence of ATF4.

392 In the present work, we found that ATF4 plays a novel role in regulating the proportion of  
393 GABA<sub>B</sub>Rs that are exposed on the neuronal surface. Two subunit isoforms of GABA<sub>B</sub> 1 receptors  
394 have been described, GABA<sub>B</sub>R 1a and GABA<sub>B</sub>R 1b, which differ by the presence of two sushi  
395 domains near the N-terminus of GABA<sub>B</sub>R 1a (Hawrot et al., 1998). Our findings indicate that ATF4

396 knockdown leads to comparable reductions of both GABA<sub>B</sub>R 1a and GABA<sub>B</sub>R 1b on the cell  
397 surface. There is evidence that GABA<sub>B</sub>R 1a subunits are mainly located presynaptically, while  
398 GABA<sub>B</sub>R 1b subunits are predominantly expressed postsynaptically (Vigot et al., 2006).  
399 Consistent with this localization and with the reductions of both subunit types on the cell surface,  
400 we observed both an increase in the frequency of mIPSCs (which is mainly a presynaptic  
401 measurement) and a decrease of GIRK currents (mainly postsynaptic in origin) after ATF4  
402 knockdown. Presynaptic GABA<sub>B</sub>Rs act as presynaptic brakes on release of neurotransmitters  
403 (Sakaba and Neher, 2003; Laviv et al., 2010) and GABA<sub>B</sub>R modulation consequently affects the  
404 frequency, but not the amplitude, of mIPSCs (Ulrich and Huguenard, 1996; Kubota et al., 2003;  
405 Kirmse and Kirischuk, 2006). Our observation that ATF4 down-regulation increases the  
406 frequency, but not amplitude, of mIPSCs is thus consistent with a decrease of pre-synaptic  
407 surface-exposed GABA<sub>B</sub>Rs. Further supporting this view, we found that application of the specific  
408 GABA<sub>B</sub>R antagonists CGP55845 and SCH50911 significantly elevated mIPSC frequency in  
409 shCtrl- but not in shATF4-treated neurons, indicating that presynaptic GABA<sub>B</sub>R activity is  
410 compromised in the ATF4 knockdown neurons.

411 Pre- and post-synaptic GABA<sub>B</sub>R function has been widely reported to be associated with G-  
412 protein inward rectifying potassium channels (GIRKs), which hyperpolarize neurons in response  
413 to GABA<sub>B</sub>R activation (Ladera et al., 2008). We therefore measured GABA<sub>B</sub>R-induced K<sup>+</sup> currents  
414 as a readout of GABA<sub>B</sub>R activity and found a 40% reduction of GIRK current in ATF4 down-  
415 regulated neurons. These observations are consistent with a decline in trafficking of post-synaptic  
416 GABA<sub>B</sub>Rs. Thus, our findings suggest effects of ATF4 on both pre- and post-synaptic GABA<sub>B</sub>Rs.  
417 Additional studies will be needed to further characterize these effects and to define their individual  
418 influences on synaptic transmission.

419 In our study, we observed that the total and surface levels of GIRK proteins were unaltered by  
420 ATF4 down-regulation; this finding suggests the idea that GABA<sub>B</sub>Rs and GIRK can be  
421 independently trafficked to the cell surface. In addition, our finding that ATF4 down-regulation  
422 reduces GABA<sub>B</sub>R functionality without affecting GABA<sub>B</sub>R 2 levels is in line with the evidence that  
423 the 2 subunits (GABA<sub>B</sub>R 1 and 2) need to heterodimerize in order to produce a functionally active  
424 GABA<sub>B</sub>R (Jones et al., 1998).

425 A major issue addressed in our study is the mechanism by which ATF4 regulates the surface  
426 expression of GABA<sub>B</sub>Rs. As a leucine zipper protein, ATF4 has the capacity to undergo direct  
427 protein-protein interactions, among which is binding to GABA<sub>B</sub>Rs. However, this interaction did  
428 not appear to be relevant to the observed regulation of GABA<sub>B</sub>R membrane trafficking since the  
429 deficits in this parameter were not rescued by a mutant ATF4 lacking DNA binding capacity, but  
430 possessing an intact leucine zipper. These observations support rather a transcriptional role for  
431 ATF4 in regulating GABA<sub>B</sub>R surface exposure. A prior study reported that ATF4 over-expression  
432 elevated expression of a GABA<sub>B</sub>R 1a promoter-reporter construct and decreased expression of a  
433 GABA<sub>B</sub>R 1b promoter-reporter construct (Steiger et al., 2004). However, we noted no changes  
434 either in GABA<sub>B</sub>R 1a or GABA<sub>B</sub>R 1b mRNA or total protein after ATF4 knockdown. Moreover,  
435 ATF4 over-expression also failed to affect surface or total GABA<sub>B</sub>R 1a or GABA<sub>B</sub>R 1b levels in  
436 our experiments. Our findings instead indicate that the role of ATF4 in controlling GABA<sub>B</sub>R  
437 trafficking stems from its transcription-dependent capacity to regulate Cdc42 expression. In

438 support of this idea, Cdc42 knockdown fully phenocopied the effects of ATF4 knockdown on  
439 surface expression of GABA<sub>B</sub>Rs. While the ATF4/Cdc42 pathway appears to be key player in  
440 GABA<sub>B</sub>R trafficking, this does not seem to be a universal mechanism for regulating receptor  
441 surface expression in neurons. Thus, ATF4 knockdown did not affect total or membrane  
442 expression of GABA<sub>B</sub>R 2, GABA<sub>A</sub> β2 and γ2 subunits, or K<sub>v</sub>1.1, K<sub>v</sub>2.1, K<sub>v</sub>4.2, and Ca<sub>v</sub>2.1 channels.  
443 It remains to be seen whether ATF4/Cdc42 pathway affects trafficking of other neurotransmitter  
444 receptors.

445 Cdc42-dependent signaling has been implicated in trafficking of GluA1 AMPA receptors (Hussain  
446 et al., 2015). One way in which the effect of Cdc42 knockdown differed from ATF4 knockdown  
447 was that the former, but not the latter caused a small, but significant increase in the amplitude of  
448 mIPSCs. One possible explanation for this discrepancy may be the different magnitude of Cdc42  
449 protein silencing exerted by the two shRNA constructs. While shATF4 caused a ~40-50%  
450 reduction of Cdc42 protein, shCdc42 depleted 70-80% of total Cdc42 protein. It may be that the  
451 greater loss of Cdc42 with shCdc42 results in post-synaptic modifications that affect GABA  
452 sensitivity.

453 Our findings establish roles for transcriptionally active ATF4 and for Cdc42 in regulation of  
454 GABA<sub>B</sub>R trafficking. Our prior work has shown that ATF4 influences Cdc42 levels by promoting  
455 its stability and that this in turn reflects the Cdc42-stabilizing activity of RhoGDIα, a direct  
456 transcriptional target of ATF4 (Pasini et al., 2016). Fig. 7 shows a proposed mechanistic pathway  
457 by which ATF4 regulates GABA<sub>B</sub>R trafficking and neuronal excitability via Cdc42 and RhoGDIα.  
458 An important feature of this mechanism is that it appears to occur over a prolonged time course.  
459 Cdc42 is a relatively stable protein and knocking down ATF4 in neurons reduces Cdc42's  
460 apparent half-life from 31.5 to 18.5 hrs (Liu et al., 2014). This suggests that sustained changes in  
461 ATF4 protein levels/activity over many hours may be required to materially affect Cdc42  
462 expression and thereby to affect synaptic activity. ATF4 itself is a rapidly turning-over protein and  
463 its expression is regulated both by translational and transcriptional mechanisms. Thus ATF4 may  
464 serve as a "sentinel" protein whose ambient expression levels in neurons influence GABA<sub>B</sub>R  
465 trafficking as well as other elements of neuronal plasticity.

466

#### 467 **Figure Legends:**

#### 468 **Figure 1:**

469 **ATF4 knockdown increases neuronal excitability. A,** The frequency of spontaneously-  
470 occurring action potentials (sAPs) is increased upon ATF4 down-regulation; this effect appears  
471 to be mediated by ATF4's transcriptional capability. Left panel, representative traces of sAPs  
472 recorded from cultured hippocampal neurons infected at DIV7 for 2 weeks with lentivirus  
473 expressing either shCtrl (black trace), shATF4 (red trace), shATF4+ATF4add (purple trace), or  
474 shATF4+ATF4add/mut (cyan trace). Right panel, summary bar graph showing the mean  
475 frequencies (± SEM) of sAPs of hippocampal neurons infected with shCtrl (black bars, n=24),  
476 shATF4 (red bars, n=22), shATF4+ATF4add (purple bars, n=18), shATF4+ATF4add/mut (cyan  
477 bars, n=18) constructs. **C-E,** ATF4 down-regulation does not affect Na<sup>2+</sup> and K<sup>+</sup> voltage-gated

478 channels in shATF4-infected neurons (red dots) when compared to shCtrl neurons (black dots).  
 479 **C**, Voltage-gated Na<sup>2+</sup> currents were evoked by 1s step depolarizations from -40 to +60 mV with  
 480 10-mV increments (shCtrl n=15; shATF4 n=16). **D**, A-type K<sup>+</sup> currents were evoked by 1s step  
 481 depolarizations from -30 to +60 mV, with 10-mV increments (shCtrl n=29; shATF4 n=33), and  
 482 successively isolated. **E**, Delayed-rectifying K<sup>+</sup> currents were evoked by 1s step depolarizations  
 483 from -90 to +60 mV, with 10 mV increments (shCtrl n=30; shATF4 n=34), and successively  
 484 isolated. Values are expressed as mean ± SEM. \*p<0.05; \*\*p<0.01.

485

486 **Figure 2:**

487 **ATF4 regulates GABA<sub>B</sub>Rs surface expression.** **A**, GABA<sub>B</sub>R blockade increases the frequency  
 488 of sAPs in control neurons. Representative trace of sAPs recorded from cultured hippocampal  
 489 neurons infected with shCtrl-carrying lentivirus treated with the specific GABA<sub>B</sub>R antagonist  
 490 CGP55845 (10 μM). **B**, Time-course experiment showing no changes in the mRNA levels for  
 491 GABA<sub>B</sub>R subunits 1a and 1b upon ATF4 down-regulation. Bar graphs represent qPCR analysis  
 492 of ATF4 (left), GABA<sub>B</sub>R 1a (center) and GABA<sub>B</sub>R 1b (right) mRNA levels extracted 4, 8, and 12  
 493 days after infection with lentivirus carrying either shCtrl (black bars) or shATF4 (red bars)  
 494 constructs. Values are expressed as mean ± SEM from three independent experiments. **C**, ATF4  
 495 down-regulation decreases membrane levels of GABA<sub>B</sub>R. *DIV7* hippocampal cultured neurons  
 496 were infected with indicated lentiviral constructs (black for shCtrl, red for shATF4, purple for  
 497 shATF4+ATF4add, and cyan for shATF4+ATF4add/mut) for 14 days before undergoing  
 498 extraction of total and membrane proteins. Left side of the panel shows a representative western  
 499 immunoblot. Bar graphs on the right portion of the panel show densitometric analysis of total (left)  
 500 or membrane (right) GABA<sub>B</sub>R 1a and 1b protein normalized to GAPDH. **D**, ATF4 down-regulation  
 501 does not affect total or surface levels of GABA<sub>B</sub>R 2. Left side of the panel shows a representative  
 502 western immunoblot. Bar graphs on the right portion of the panel show densitometric analysis of  
 503 total (left) or membrane (right) GABA<sub>B</sub>R 2 protein normalized to GAPDH. Values are expressed  
 504 as mean ± SEM from three independent experiments. \*p<0.05. \*\*p<0.01; \*\*\*p<0.001.

505

506 **Figure 3:**

507 **ATF4 down-regulation does not affect total and membrane levels of GABA<sub>A</sub>Rs and voltage-**  
 508 **sensitive K or Ca channels.** *DIV7* cultured hippocampal neurons were infected with indicated  
 509 lentiviral constructs (black for shCtrl, red for shATF4) for 14 days before undergoing extraction of  
 510 total and membrane proteins. **A**, Left side of the panel shows a representative western  
 511 immunoblot. Bar graphs show densitometric analysis of total (left) or membrane (right) GABA<sub>A</sub>R  
 512 β2 and γ2 protein normalized to GAPDH. **B**, Upper panel shows a representative western  
 513 immunoblot. Bar graphs show densitometric analysis of total (left) or membrane (right) K<sub>v</sub>1.1  
 514 protein normalized to GAPDH. **C**, Upper panel shows a representative western immunoblot. Bar  
 515 graphs show densitometric analysis of total (left) or membrane (right) K<sub>v</sub>2.1 protein normalized to  
 516 GAPDH. **D**, Upper panel shows a representative western immunoblot. Bar graphs show  
 517 densitometric analysis of total (left) or membrane (right) K<sub>v</sub>4.2 protein normalized to GAPDH. **E**,

518 Upper panel shows a representative western immunoblot. Bar graphs show densitometric  
 519 analysis of total (left) or membrane (right)  $Ca_v2.1$  protein normalized to GAPDH. Values are  
 520 expressed as mean  $\pm$  SEM from three independent experiments, each run in duplicate. The  
 521 differences between shCtrl and shATF4 were not significant ( $p>0.05$ ) in all cases.

522

523 **Figure 4:**

524 **ATF4 knockdown reduces GABA<sub>B</sub>R-induced GIRK currents.** **A**, Specific GABA<sub>B</sub>R agonist  
 525 Baclofen (100  $\mu$ M) elicited a sustained GIRK current in cultured hippocampal neurons infected  
 526 with shCtrl lentivirus (top panel shows a representative trace). This effect is abolished by  
 527 pretreating the culture with the specific GABA<sub>B</sub>R antagonist CGP55845 (10  $\mu$ M; bottom panel).  
 528 **B**, shATF4 infection reduces Baclofen-induced GIRK currents; this effect is dependent on ATF4's  
 529 transcriptional capability. Left panel shows representative traces of Baclofen-elicited currents  
 530 recorded from *DIV7* cultured hippocampal neurons infected for two weeks with lentivirus  
 531 expressing either shCtrl (black), shATF4 (red), shATF4+ATF4add (purple), or  
 532 shATF4+ATF4add/mut (cyan). Bar graphs on the right indicate measurements of the currents  
 533 (shCtrl n=37; shATF4 n=39; shATF4+ATF4add n=36; shATF4+ATF4add/mut n=51). Values are  
 534 expressed as mean  $\pm$  SEM. \* $p<0.05$ ; \*\* $p<0.005$ . **C**, ATF4 down-regulation does not affect total  
 535 and membrane levels of GIRK proteins. *DIV7* cultured hippocampal neurons were infected with  
 536 indicated lentiviral constructs (black for shCtrl, red for shATF4) for 14 days before undergoing  
 537 extraction of total and membrane proteins. Left side of the panel shows a representative western  
 538 immunoblot. Bar graphs show densitometric analysis of total (left) or membrane (right) GIRK  
 539 proteins normalized to GAPDH. Values are expressed as mean  $\pm$  SEM from three independent  
 540 experiments. \* $p<0.05$ . \*\* $p<0.01$ ; \*\*\* $p<0.001$ .

541

542 **Figure 5:**

543 **ATF4 knockdown increases the frequency, but not amplitude of mIPSCs.** **A**, Left portion of  
 544 the panel shows representative mIPSC traces recorded from *DIV7* hippocampal neurons infected  
 545 for two weeks with lentivirus expressing either shCtrl (black), shATF4 (red), shATF4+ATF4add  
 546 (purple), or shATF4+ATF4add/mut (cyan). On the right portion of the panel, bar graphs quantify  
 547 the frequency (left) and the amplitude (right) of mIPSCs shown in A. (shCtrl, n=46; shATF4, n=29;  
 548 shATF4+ATF4add, n=16; shATF4+ATF4add/mut, n=25). Values are expressed as mean  $\pm$  SEM.  
 549 **B**, Effect of pharmacological manipulation of GABA<sub>B</sub>R on mIPSCs recorded from *DIV7*  
 550 hippocampal neurons infected for two weeks with lentivirus expressing either shCtrl, or shATF4.  
 551 Top panel shows representative traces of mIPSCs recorded from shCtrl (black traces) or shATF4  
 552 (red traces) infected neurons alone (shCtrl, n=49; shATF4, n=29) or in the presence of either 20  
 553  $\mu$ M Baclofen (GABA<sub>B</sub>R agonist; shCtrl, n=16; shATF4, n=15), 10  $\mu$ M SCH50911 (GABA<sub>B</sub>R  
 554 antagonist; shCtrl, n=36; shATF4, n=18), or 100  $\mu$ M CGP55845 (GABA<sub>B</sub>R antagonist; shCtrl,  
 555 n=21; shATF4, n=17). In the bottom portion of the panel, bar graphs quantify the frequency (left)  
 556 and the amplitude (right) of the mIPSCs. Values are expressed as mean  $\pm$  SEM. \* indicates  
 557  $p<0.05$ ; \*\* indicates  $p<0.01$ ; \*\*\* indicates  $p<0.001$ .

558

559 **Figure 6:**

560 **The effects of ATF4 on excitability and GABA<sub>B</sub>Rs are driven by changes in Cdc42**  
561 **expression. A,** Cdc42 down-regulation increases intrinsic neuronal excitability. Top panel shows  
562 representative traces of sAPs recorded from cultured hippocampal neurons infected at *DIV7* for  
563 2 weeks with lentivirus expressing either shCtrl (black trace) or shCdc42 (blue trace). Bottom  
564 panel shows summary bar graphs showing the frequency of sAPs of neurons infected with shCtrl  
565 (black bars, n=13) or shCdc42 (blue bars, n=13) constructs. **B,** Cdc42 down-regulation decreases  
566 membrane but not total GABA<sub>B</sub>R levels. *DIV7* cultured hippocampal neurons were infected with  
567 different lentiviral constructs (black for shCtrl, blue for shCdc42) for two weeks before undergoing  
568 extraction of total and membrane proteins. Left portion of the panel shows a representative  
569 Western immunoblot. Bar graphs on the right portion of the panel show densitometric analysis of  
570 immunoblots for total (left) or membrane (right) GABA<sub>B</sub>R 1a and 1b protein, normalized to  
571 GAPDH. **C,** Cdc42 down-regulation decreases Baclofen-elicited GIRK currents. Top side of the  
572 panel shows representative traces of Baclofen-elicited currents recorded from *DIV7* cultured  
573 hippocampal neurons infected for two weeks with lentivirus carrying either shCtrl (black) or  
574 shCdc42 (blue). Bar graph on the bottom side shows the measurements of the currents (shCtrl,  
575 n=22; shCdc42, n=26). **D,** Cdc42 down-regulation increases mIPSCs. Top portion of the panel  
576 shows representative mIPSC traces recorded from *DIV7* hippocampal neurons infected for two  
577 weeks with lentivirus carrying either shCtrl (black) or shCdc42 (blue) constructs. On the bottom  
578 portion of the panel, bar graphs quantify the frequency (left) and the amplitude (right) of mIPSCs  
579 shown in A. (shCtrl, n=34; shCdc42, n=29). Values are expressed as mean ± SEM. \* indicates  
580 p<0.05.

581

582 **Figure 7:**

583 **Proposed mechanism by which ATF4 regulates neuronal excitability.** Left panel shows a  
584 control condition where basal levels of ATF4 protein ensure the appropriate amount of RhoGDI $\alpha$   
585 expression to bind and stabilize cytoplasmic Rho GTPase family members, including Cdc42.  
586 Appropriate levels of Cdc42 result in basal levels of membrane-bound GABA<sub>B</sub>Rs that contribute  
587 to control the pace of neuronal firing. The right side of the panel shows a condition of chronic  
588 ATF4 down regulation, the consequent decrease of RhoGDI $\alpha$  levels and augmented Cdc42  
589 turnover. This in turn negatively affects the amount of membrane-bound GABA<sub>B</sub>Rs, altering  
590 neuronal intrinsic excitability properties, which results in increased sAP frequency.

591

592 **References:**

593

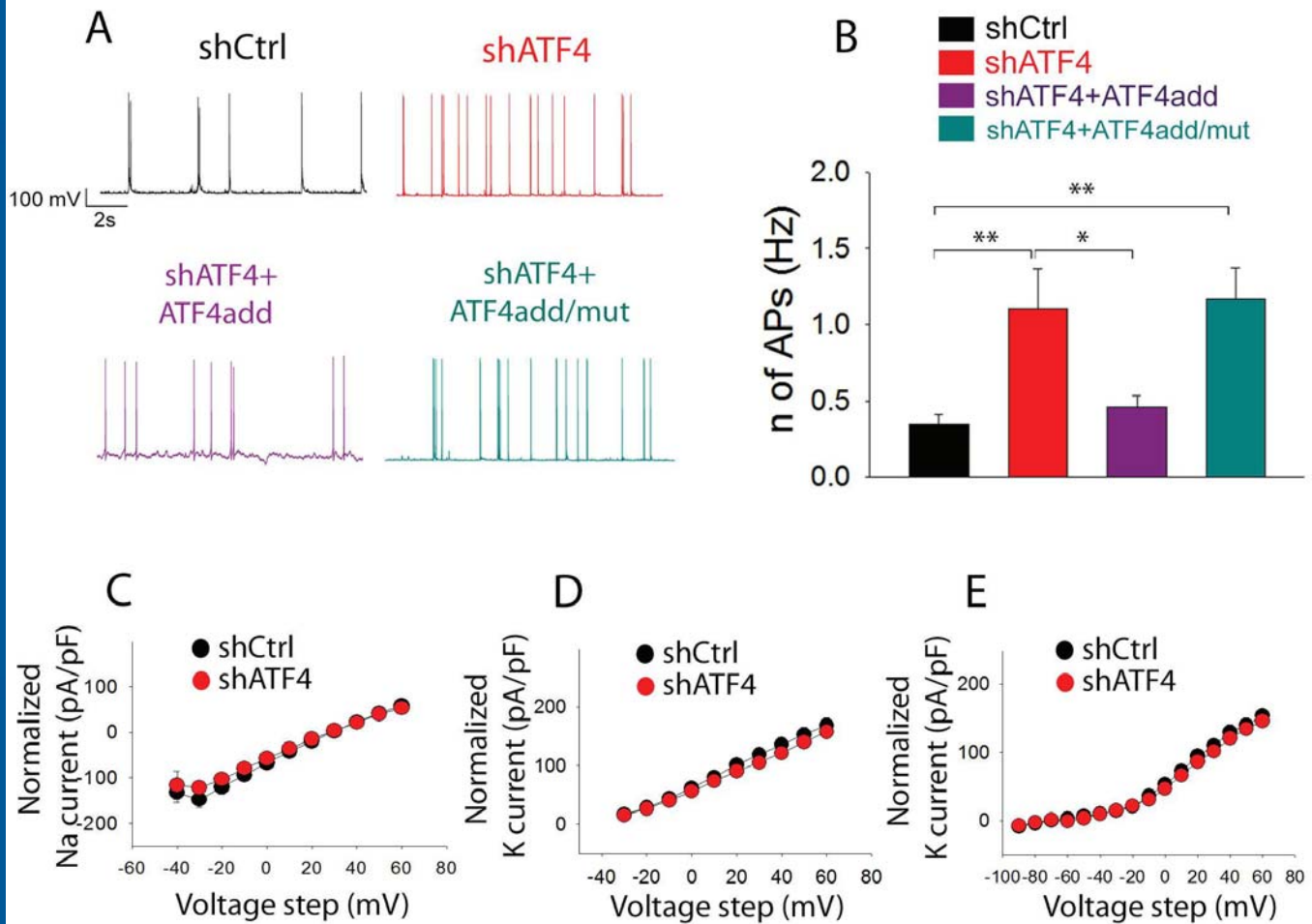
594 Ameri K, Harris AL (2008) Activating transcription factor 4. *Int J Biochem Cell Biol* 40:14-21.

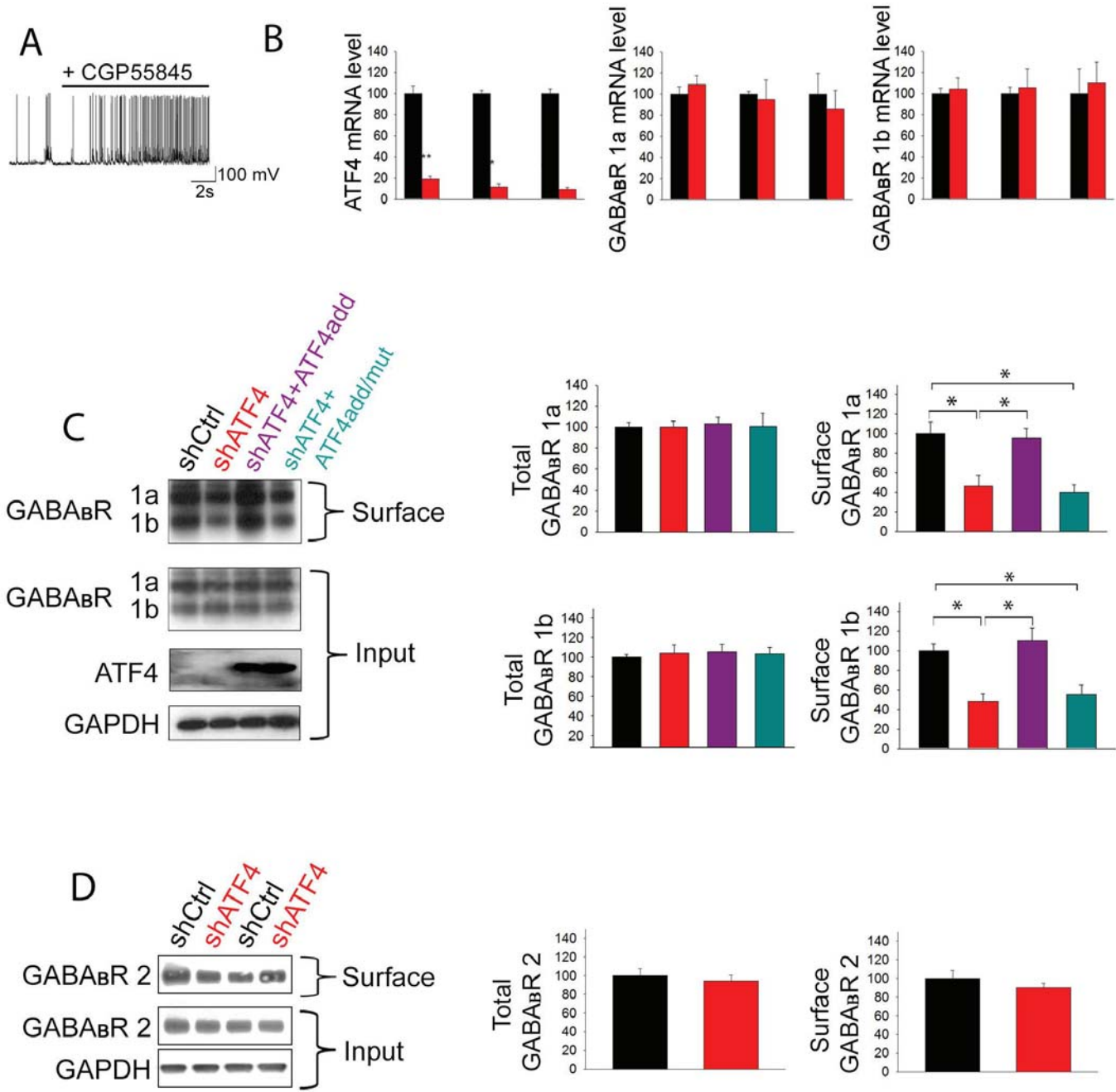


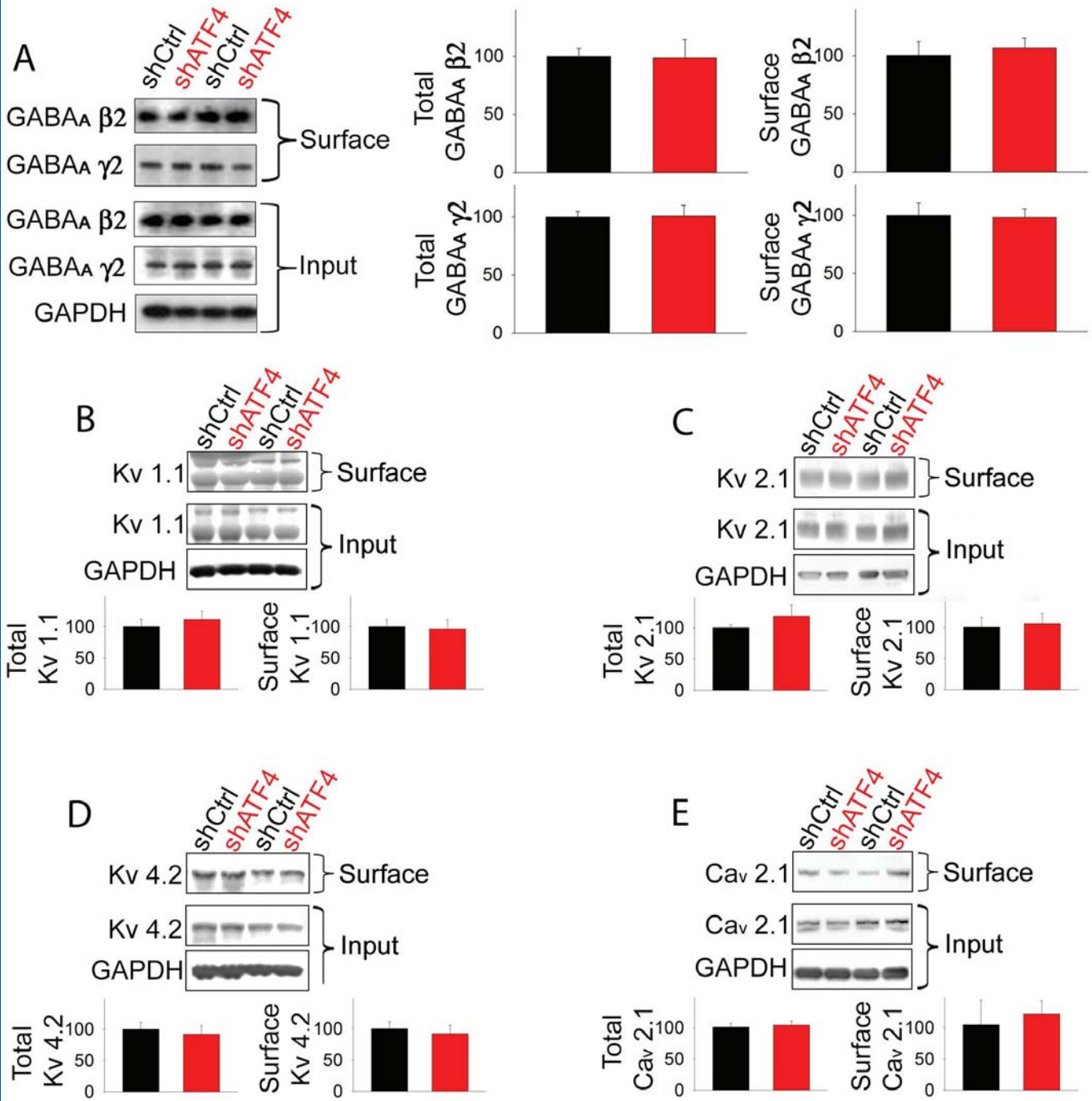
- 595 Bartsch D, Ghirardi M, Skehel PA, Karl KA, Herder SP, Chen M, Bailey CH, Kandel ER (1995) Aplysia CREB2  
596 represses long-term facilitation: relief of repression converts transient facilitation into long-term  
597 functional and structural change. *Cell* 83:979-992.
- 598 Bean BP (2007) The action potential in mammalian central neurons. *Nat Rev Neurosci* 8:451-465.
- 599 Beck H, Yaari Y (2008) Plasticity of intrinsic neuronal properties in CNS disorders. *Nat Rev Neurosci*  
600 9:357-369.
- 601 Chen A, Muzzio IA, Malleret G, Bartsch D, Verbitsky M, Pavlidis P, Yonan AL, Vronskaya S, Grody MB,  
602 Cepeda I, Gilliam TC, Kandel ER (2003) Inducible enhancement of memory storage and synaptic  
603 plasticity in transgenic mice expressing an inhibitor of ATF4 (CREB-2) and C/EBP proteins.  
604 *Neuron* 39:655-669.
- 605 Chen X, Yuan LL, Zhao C, Birnbaum SG, Frick A, Jung WE, Schwarz TL, Sweatt JD, Johnston D (2006)  
606 Deletion of Kv4.2 gene eliminates dendritic A-type K<sup>+</sup> current and enhances induction of long-  
607 term potentiation in hippocampal CA1 pyramidal neurons. *J Neurosci* 26:12143-12151.
- 608 Costa-Mattioli M, Gobert D, Stern E, Gamache K, Colina R, Cuellar C, Sossin W, Kaufman R, Pelletier J,  
609 Rosenblum K, Krnjevic K, Lacaille JC, Nader K, Sonenberg N (2007) eIF2 $\alpha$  phosphorylation  
610 bidirectionally regulates the switch from short- to long-term synaptic plasticity and memory. *Cell*  
611 129:195-206.
- 612 Gassmann M, Bettler B (2012) Regulation of neuronal GABA(B) receptor functions by subunit  
613 composition. *Nat Rev Neurosci* 13:380-394.
- 614 Hawrot E, Xiao Y, Shi QL, Norman D, Kirkitadze M, Barlow PN (1998) Demonstration of a tandem pair of  
615 complement protein modules in GABA(B) receptor 1a. *FEBS Lett* 432:103-108.
- 616 Hsiao CF, Kaur G, Vong A, Bawa H, Chandler SH (2009) Participation of Kv1 channels in control of  
617 membrane excitability and burst generation in mesencephalic V neurons. *J Neurophysiol*  
618 101:1407-1418.
- 619 Hu JY, Levine A, Sung YJ, Schacher S (2015) cJun and CREB2 in the postsynaptic neuron contribute to  
620 persistent long-term facilitation at a behaviorally relevant synapse. *J Neurosci* 35:386-395.
- 621 Hussain NK, Thomas GM, Luo J, Haganir RL (2015) Regulation of AMPA receptor subunit GluA1 surface  
622 expression by PAK3 phosphorylation. *Proc Natl Acad Sci U S A* 112:E5883-5890.
- 623 Jones KA, Borowsky B, Tamm JA, Craig DA, Durkin MM, Dai M, Yao WJ, Johnson M, Gunwaldsen C,  
624 Huang LY, Tang C, Shen Q, Salon JA, Morse K, Laz T, Smith KE, Nagarathnam D, Noble SA,  
625 Branchek TA, Gerald C (1998) GABA(B) receptors function as a heteromeric assembly of the  
626 subunits GABA(B)R1 and GABA(B)R2. *Nature* 396:674-679.
- 627 Kim IH, Wang H, Soderling SH, Yasuda R (2014) Loss of Cdc42 leads to defects in synaptic plasticity and  
628 remote memory recall. *Elife* 3.
- 629 Kirmse K, Kirischuk S (2006) Ambient GABA constrains the strength of GABAergic synapses at Cajal-  
630 Retzius cells in the developing visual cortex. *J Neurosci* 26:4216-4227.
- 631 Kubota H, Katsurabayashi S, Moorhouse AJ, Murakami N, Koga H, Akaike N (2003) GABAB receptor  
632 transduction mechanisms, and cross-talk between protein kinases A and C, in GABAergic  
633 terminals synapsing onto neurons of the rat nucleus basalis of Meynert. *J Physiol* 551:263-276.
- 634 Ladera C, del Carmen Godino M, Jose Cabanero M, Torres M, Watanabe M, Lujan R, Sanchez-Prieto J  
635 (2008) Pre-synaptic GABA receptors inhibit glutamate release through GIRK channels in rat  
636 cerebral cortex. *J Neurochem* 107:1506-1517.
- 637 Laviv T, Riven I, Dolev I, Vertkin I, Balana B, Slesinger PA, Slutsky I (2010) Basal GABA regulates GABA(B)R  
638 conformation and release probability at single hippocampal synapses. *Neuron* 67:253-267.
- 639 Leung LS, Peloquin P (2006) GABA(B) receptors inhibit backpropagating dendritic spikes in hippocampal  
640 CA1 pyramidal cells in vivo. *Hippocampus* 16:388-407.
- 641 Liu J, Pasini S, Shelanski ML, Greene LA (2014) Activating transcription factor 4 (ATF4) modulates post-  
642 synaptic development and dendritic spine morphology. *Front Cell Neurosci* 8:177.

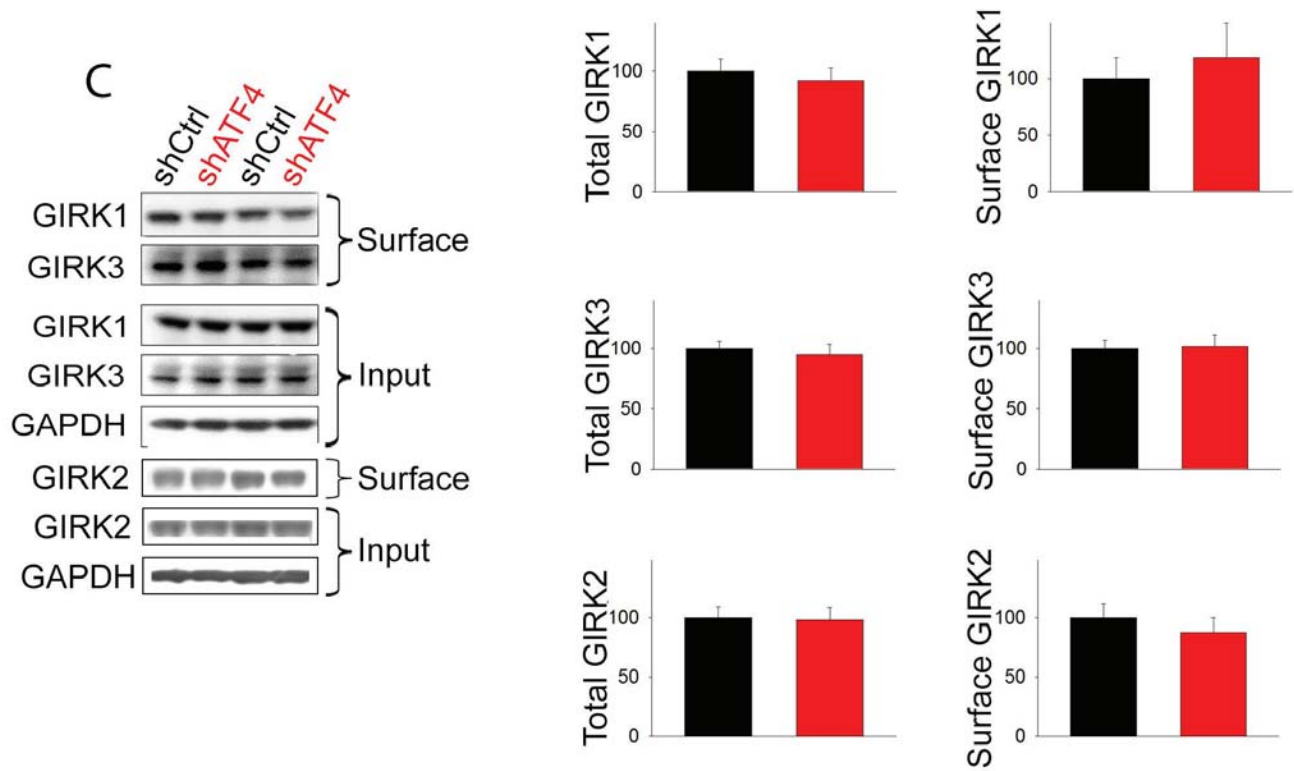
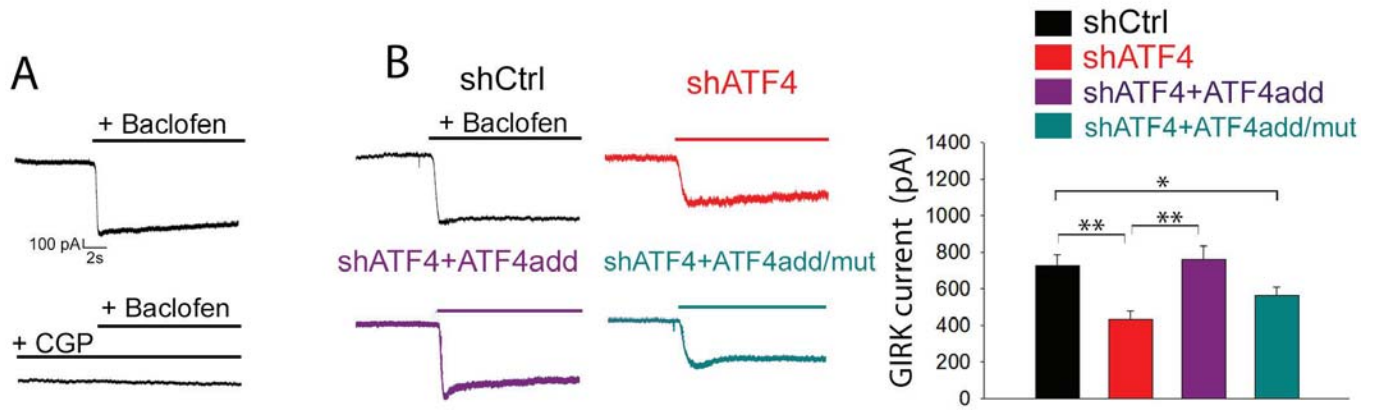
- 643 Nehring RB, Horikawa HP, El Far O, Kneussel M, Brandstatter JH, Stamm S, Wischmeyer E, Betz H,  
644 Karschin A (2000) The metabotropic GABAB receptor directly interacts with the activating  
645 transcription factor 4. *J Biol Chem* 275:35185-35191.
- 646 Pasini S, Corona C, Liu J, Greene LA, Shelanski ML (2015) Specific downregulation of hippocampal ATF4  
647 reveals a necessary role in synaptic plasticity and memory. *Cell Rep* 11:183-191.
- 648 Pasini S, Liu J, Corona C, Peze-Heidsieck E, Shelanski M, Greene LA (2016) Activating Transcription Factor  
649 4 (ATF4) modulates Rho GTPase levels and function via regulation of RhoGDIalpha. *Sci Rep*  
650 6:36952.
- 651 Ritter B, Zschuntsch J, Kvachnina E, Zhang W, Ponimaskin EG (2004) The GABA(B) receptor subunits R1  
652 and R2 interact differentially with the activation transcription factor ATF4 in mouse brain during  
653 the postnatal development. *Brain Res Dev Brain Res* 149:73-77.
- 654 Rossignol E, Kruglikov I, van den Maagdenberg AM, Rudy B, Fishell G (2013) CaV 2.1 ablation in cortical  
655 interneurons selectively impairs fast-spiking basket cells and causes generalized seizures. *Ann*  
656 *Neurol* 74:209-222.
- 657 Sakaba T, Neher E (2003) Direct modulation of synaptic vesicle priming by GABA(B) receptor activation  
658 at a glutamatergic synapse. *Nature* 424:775-778.
- 659 Speca DJ, Ogata G, Mandikian D, Bishop HI, Wiler SW, Eum K, Wenzel HJ, Doisy ET, Matt L, Campi KL,  
660 Golub MS, Nerbonne JM, Hell JW, Trainor BC, Sack JT, Schwartzkroin PA, Trimmer JS (2014)  
661 Deletion of the Kv2.1 delayed rectifier potassium channel leads to neuronal and behavioral  
662 hyperexcitability. *Genes Brain Behav* 13:394-408.
- 663 Steiger JL, Bandyopadhyay S, Farb DH, Russek SJ (2004) cAMP response element-binding protein,  
664 activating transcription factor-4, and upstream stimulatory factor differentially control  
665 hippocampal GABABR1a and GABABR1b subunit gene expression through alternative  
666 promoters. *J Neurosci* 24:6115-6126.
- 667 Ulrich D, Huguenard JR (1996) Gamma-aminobutyric acid type B receptor-dependent burst-firing in  
668 thalamic neurons: a dynamic clamp study. *Proc Natl Acad Sci U S A* 93:13245-13249.
- 669 Vernon E, Meyer G, Pickard L, Dev K, Molnar E, Collingridge GL, Henley JM (2001) GABA(B) receptors  
670 couple directly to the transcription factor ATF4. *Mol Cell Neurosci* 17:637-645.
- 671 Vigot R, Barbieri S, Brauner-Osborne H, Turecek R, Shigemoto R, Zhang YP, Lujan R, Jacobson LH,  
672 Biermann B, Fritschy JM, Vacher CM, Muller M, Sansig G, Guetg N, Cryan JF, Kaupmann K,  
673 Gassmann M, Oertner TG, Bettler B (2006) Differential compartmentalization and distinct  
674 functions of GABAB receptor variants. *Neuron* 50:589-601.
- 675 White JH, McIlhinney RA, Wise A, Ciruela F, Chan WY, Emson PC, Billinton A, Marshall FH (2000) The  
676 GABAB receptor interacts directly with the related transcription factors CREB2 and ATFx. *Proc*  
677 *Natl Acad Sci U S A* 97:13967-13972.
- 678 Zapata J et al. (2017) Epilepsy and intellectual disability linked protein Shrm4 interaction with GABABRs  
679 shapes inhibitory neurotransmission. *Nat Commun* 8:14536.

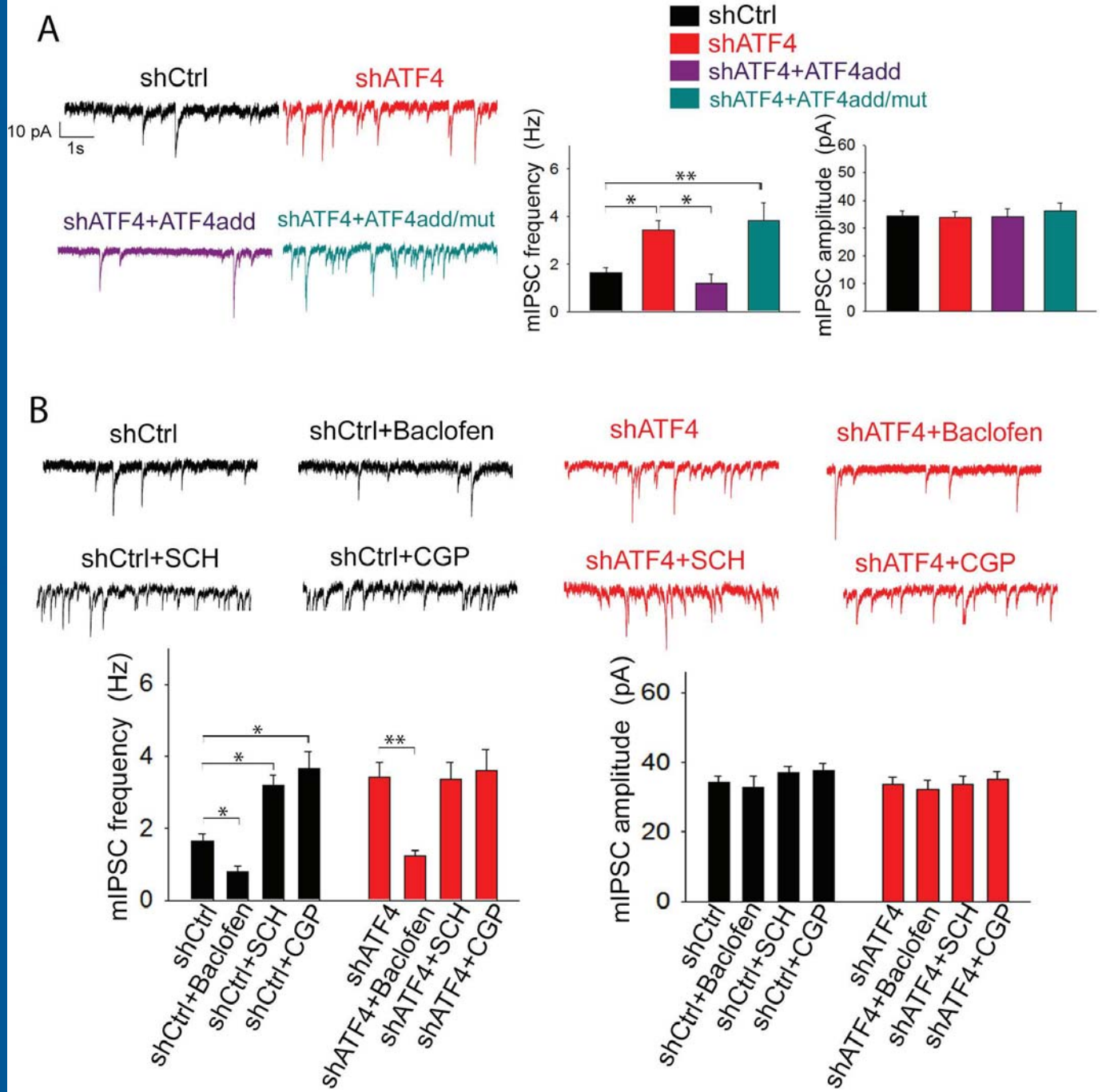
680

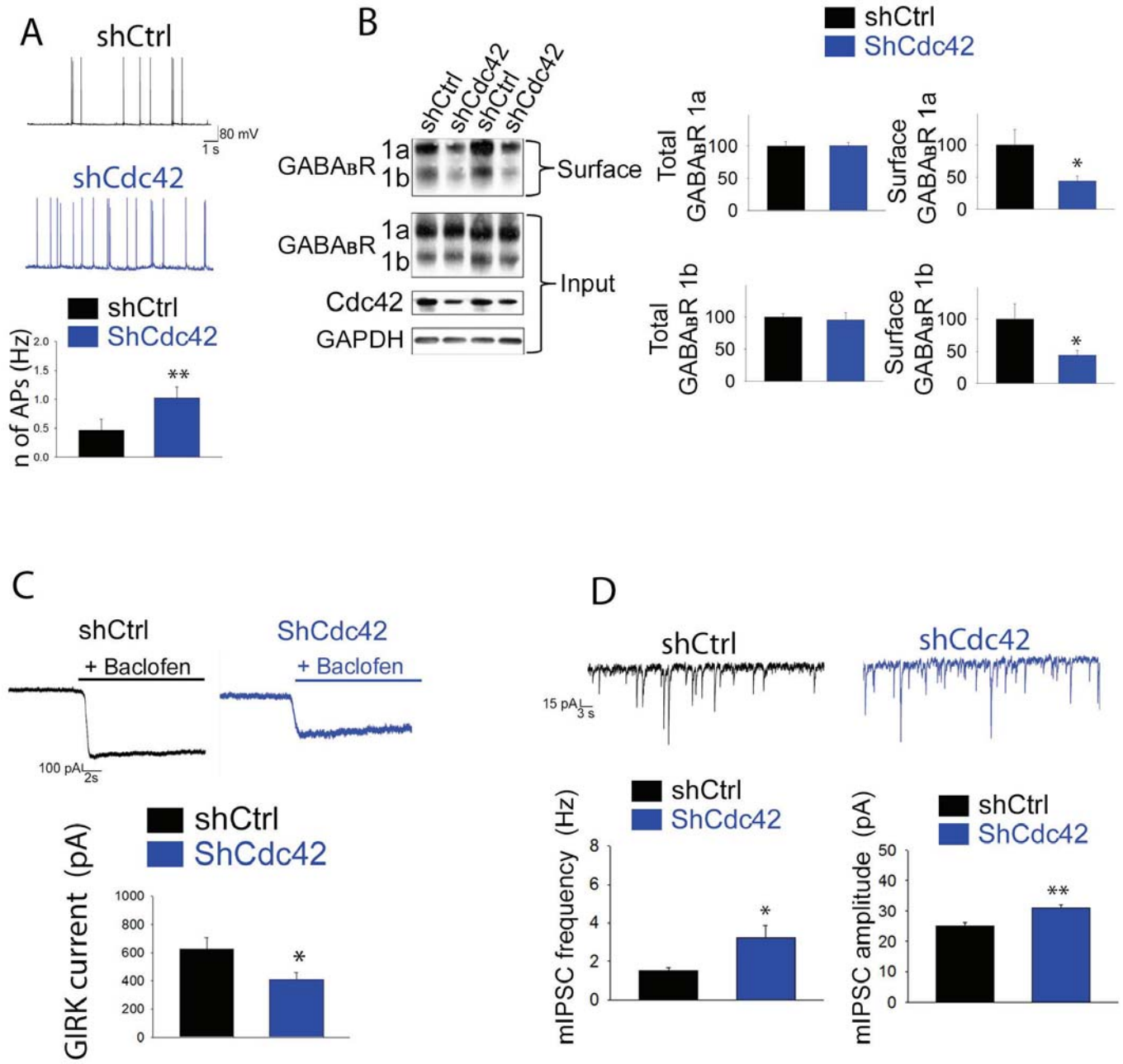






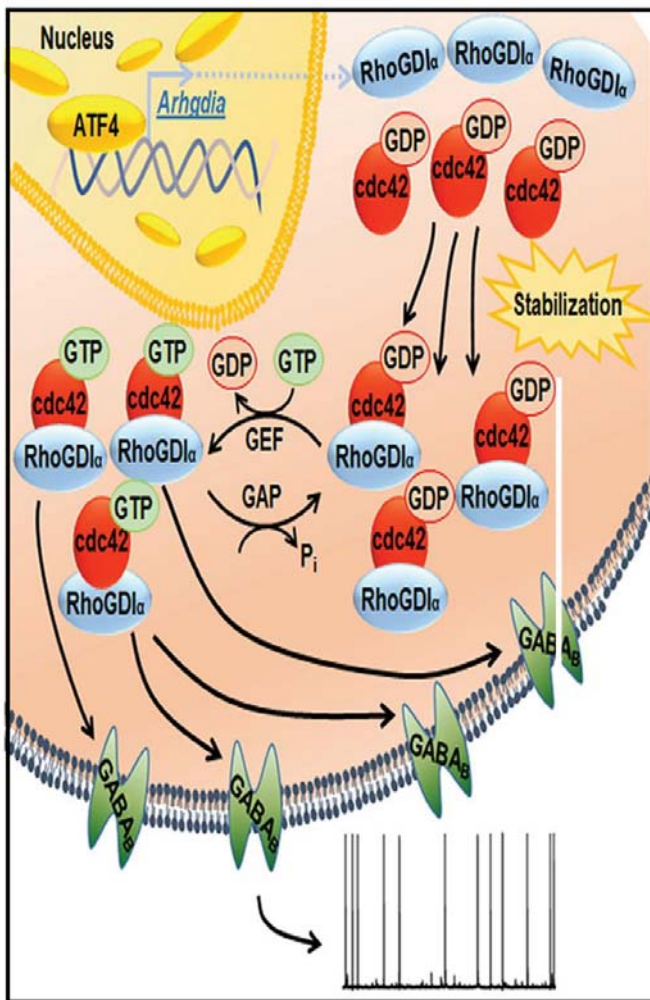








# Control



# Chronic ATF4 down-regulation

